PARTICLE SIMULATIONS OF A LONG PULSE ELECTRON BEAM IN A BEND

B. R. Poole, Y. –J. Chen

Lawrence Livermore National Laboratory, Livermore, CA 94550, USA

Abstract

Advanced x-ray radiography machines require that multiple electron beam pulses be delivered to x-ray converter targets over several lines of sight. This can be accomplished using a single accelerator by using a fast kicker to deliver the electron beam pulses to several beamlines. This type of radiography machine requires transport lines with several large achromatic bends in the individual transport lines. To maintain a small spot size and a large dose for an x-ray pulse created at the converter target at each transport line requires that emittance growth be kept to a minimum on each beamline. Emittance growth can arise from nonlinear forces associated with the external focusing elements, nonlinear image forces, and non-linear space charge fields associated with the curvature of the beam and the transport line. We have used a multi-slice, particle-in-cell code to study the emittance growth in a bend. The code uses the beam slice's local coordinates. Typically, the radius of curvature, R for such a beam and the transport line is much larger than the pipe radius, b. The space charge fields can be approximated as that in a straight beam with correction terms to first order in b/R. To include the effects of the bend geometry on the space charge fields, these correction terms are implemented in the code. The relative importance of emittance growth due to nonlinear image forces associated with envelope oscillations of a non-round beam in the bend and due to nonlinear space charge fields associated with the bend geometry will be quantified. Simulation results for the baseline design orbit as well as off-energy transport will be presented.

1 INTRODUCTION

Multi-axis radiography machines using a single LINAC as an electron beam source will, by necessity, contain several large angle bends to deliver individual electron beam pulses to several x-ray converter targets. The performance of these machines requires that a small time integrated spot size be maintained on the x-ray target for the beam pulse. This requirement directly translates to minimizing the emittance growth in the post-accelerator transport for each transport line. Each beam transport line will contain a set of magnetic focusing elements and fast beam kickers as well as large angle bends which will direct the beam pulse to the appropriate x-ray converter target. Particle-in-cell (PIC) code simulations have proved to be a useful design tool for the second axis of the Dual Axis Radiographic Hydrodynamic Test Facility (DARHT-II) [1]. In this paper we discuss the use of PIC modelling to estimate emittance growth in large angle bends due to nonlinear space charge fields associated with the curvature of the beam and transport line as well as due to nonlinear image forces associated with envelope oscillations.

An analytic model for determining the space charge forces experienced by a round beam in a continuous bend has been developed previously [2]. The results of this model are incorporated into a PIC code to estimate emittance growth due to the nonlinear space charge forces. In addition, nonlinear image forces due to envelope oscillations associated with transport in an achromatic bend can lead to emittance growth. These terms are also estimated using a PIC code.

2 MODELLING

2.1 Nonlinear Space Charge Fields

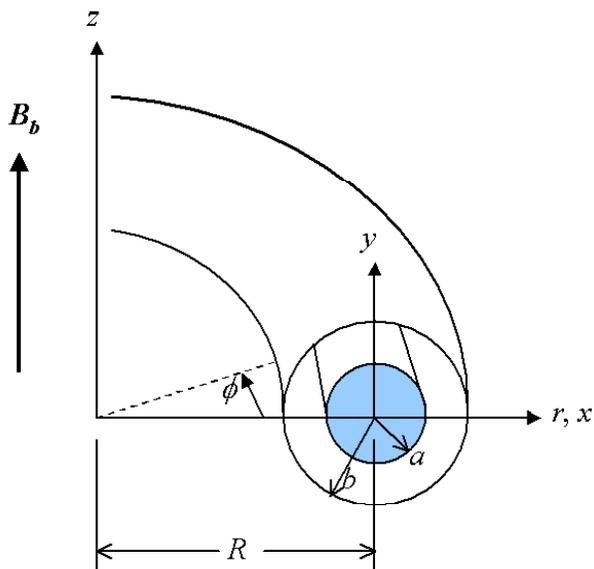Figure 1 shows the geometry for the round beam in a continuous bend.

Figure 1: Round beam in a continuous bend

The equations of motion for a charge q are given by equations 1 through 5.

$$\gamma \frac{dv_r}{dt} = \gamma \frac{v_\phi^2}{r} - v_r \frac{d\gamma}{dt} + \frac{F_r}{m} \qquad (1)$$

$$\gamma \frac{dv_\phi}{dt} = -\gamma \frac{v_r v_\phi}{r} - v_\phi \frac{d\gamma}{dt} + \frac{F_\phi}{m} \qquad (2)$$

$$\gamma \frac{dv_z}{dt} = -v_z \frac{d\gamma}{dt} + \frac{F_z}{m} \qquad (3)$$

$$\frac{d\gamma}{dt} = -\frac{q}{mc^2} \mathbf{v} \cdot \nabla \Phi \qquad (4)$$

$$\mathbf{F} = q\frac{\mathbf{v}}{c} \times \mathbf{B_b} - q\nabla\Phi + q\frac{\mathbf{v}}{c} \times (\nabla \times \mathbf{A}) \qquad (5)$$

$\mathbf{B_b}$ is the external bend magnetic field, and Φ and $\mathbf{A}$ are the electric potential and magnetic vector potential associated with the beam space charge fields. It is assumed that $\partial/\partial\phi = 0$. The electric potential, Φ and the magnetic vector potential, $\mathbf{A}$ are determined from

$$\nabla^2 \Phi(r,z) = -4\pi\rho(r,z) \qquad (6)$$

$$\nabla^2 A_\phi(r,z) - \frac{A_\phi^2(r,z)}{r^2} = -4\pi\rho(r,z)\beta_\phi(r,z) \quad (7)$$

For sufficiently high energy beams the variation in particle velocity, β_ϕ throughout the beam is negligible. Both the electric potential and magnetic vector potential vanish on the beamline wall. By writing the magnetic vector potential in the following form

$$A_\phi(r,z) = \beta_\phi \Phi(r,z) + \delta A_\phi(r,z) \qquad (8)$$

an equation for δA_ϕ can be written as

$$\nabla^2 \delta A_\phi(r,z) = \frac{\beta_\phi \Phi(r,z)}{r^2} \qquad (9)$$

which is second order in a/r. δA_ϕ vanishes on the beamline wall. The particle dynamical equations are expressed in terms of the beam's local coordinates, ($x = r - R$, $y = z$, $s = -R\phi$). The ideal beam orbit is defined by:

$$r = R, \quad \left(\frac{\gamma_w v_\phi c}{R} + \frac{qB_b}{m} \right) = 0 \qquad (10)$$

and the equations of motion become

$$\frac{(\gamma\beta_s)'}{\gamma\beta_s} x' - \frac{x'^2}{x+R} + x'' =$$

$$+ \frac{q}{\gamma\beta_s mc}\left(\frac{x+R}{R}\right)\left[\left(\frac{x+R}{R}\right)\frac{E_x}{\beta_s c}\right.$$

$$\left. -\left(\frac{x+R}{R}\right)B_y + y'B_s\right] + \frac{x+R}{R^2} \qquad (11)$$

$$\frac{(\gamma\beta_s)'}{\gamma\beta_s} y' - \frac{x'y'}{x+R} + y'' =$$

$$+ \frac{q}{\gamma\beta_s mc}\left(\frac{x+R}{R}\right)\left[\left(\frac{x+R}{R}\right)\frac{E_y}{\beta_s c}\right.$$

$$\left. +\left(\frac{x+R}{R}\right)B_x - x'B_s\right] \qquad (12)$$

$$\gamma' = \frac{q}{m}\left[x'E_x + y'E_y + \left(\frac{x+R}{R}\right)E_s\right] \qquad (13)$$

Equations 6 through 13 are implemented in a PIC code to provide an estimate of emittance growth due to nonlinear space charge effects in a bend. Equation 14 provides an estimate of the normalized emittance growth due to the curvature of the beam [2]

$$\Delta\varepsilon = \frac{\sqrt{2}}{8}\frac{I}{\beta_\phi I_0}\frac{a^2}{R}\alpha_b \qquad (14)$$

where I is the beam current, $I_0 = mc^3/e = 17$ kA, a is the beam radius, R is the bend radius, and α_b is the bend angle.

As an example we calculate the emittance growth in a 45 degree 1.08 kG bending magnet. The beam pipe radius is 8 cm and the radius of curvature of the 20 MeV, 2 kA beam is approximately 63 cm. Figure 2 shows the initial transverse beam phase space for an initial beam diverging with a angle of approximately 6 mr and has a radius of approximately 2.4 cm as shown in Fig. 2. The normalized emittance is 1200 mm-mr. Figure 3 shows the normalized emittance growth from the PIC code compared with the analytic estimate from equation 14.
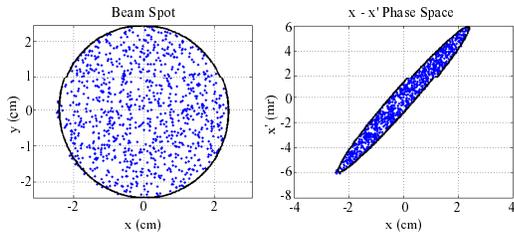
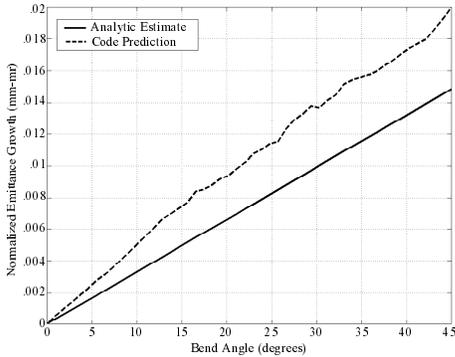Figure 2: Initial transverse phase space of beam entering a 45 degree bend

Figure 3: Emittance growth from nonlinear space charge forces in 45 degree bend

2.2 Nonlinear Image Forces

Figure 4 shows an example of a simple achromatic bend for a 20 MeV beam consisting of two 45 degree bending magnets and several quadrupoles that produces substantial envelope oscillations of the beam as shown from the TRANSPORT simulation shown in Figure 5.
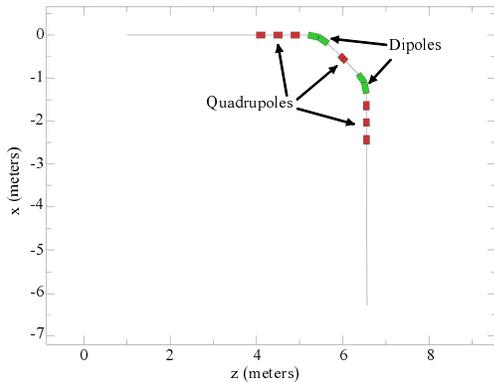

Figure 4: Simple 20 MeV achromatic bend

The envelope oscillations can be a source of emittance growth due to nonlinear image forces. The initial un-normalized emittance is 3 cm-mr and Figure 6 shows the transverse phase space in y in the vicinity of the next to the last quadrupole where the beam is large and highly elliptical. The outer edges of the beam are experiencing an octupole image field leading to a curvature of the phase space and an emittance growth of approximately 8%.
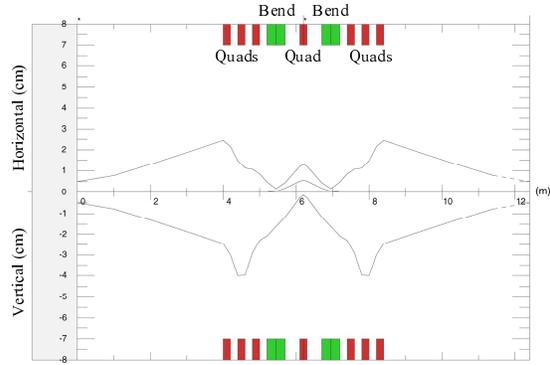

Figure 5: Strong envelope oscillations are present in 20 MeV achromatic bend can lead to emittance growth
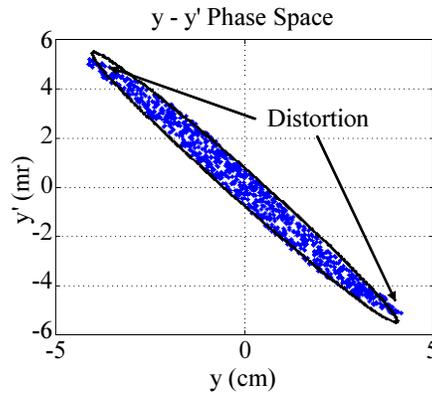

Figure 6: Phase space distortion due to image force

3 CONCLUSIONS

Estimates of emittance growth in an achromatic bend due to nonlinear space charge fields associated with the beam curvature have been made with a PIC code and found to be consistent with analytic estimates. Emittance growth due to nonlinear image forces associated with envelope oscillations have also been studied using a PIC code and found to dominate the emittance growth in the bend.

4 ACKNOWLEDGEMENTS

REFERENCES

[1] B. R. Poole, Y. –J. Chen, Y. J. (Judy) Chen, A. C. Paul, L. –F. Wang, "Particle Simulation of DARHT-II Downstream Transport", LINAC'2000, Monterey, August 2000.

[2] Y. –J. Chen, "Space Charge Forces of a DC Beam in a Continuous Bend", PAC'97, Vancouver, May 1997.